

Effect of $\text{CaF}_2/\text{P}_2\text{O}_5$ ratios on physical and mechanical properties of novel $\text{CaO-Na}_2\text{O-B}_2\text{O}_3\text{-SiO}_2$ glasses

Zhi Wei Loh^a, Mohd Hafiz Mohd Zaid^{a,b,*}, Mohd Mustafa Awang Kechik^a, Yap Wing Fen^a, Yazid Yaakob^{a,c}, Mohd Zul Hilmi Mayzan^d, Shahira Liza^e, Wei Mun Cheong^a

^a Department of Physics, Faculty of Science, Universiti Putra Malaysia, UPM., 43400 Serdang, Selangor, Malaysia

^b Nanomaterials Synthesis and Characterization Laboratory (NSCL), Institute of Nanoscience and Nanotechnology (ION2), Universiti Putra Malaysia, 43400 UPM Serdang, Selangor, Malaysia

^c Department of Physical Science and Engineering, Graduate School of Engineering, Nagoya Institute of Technology, Gokiso-cho, Showa-ku, Nagoya, 466-8555, Japan

^d Ceramic and Amorphous Group (CerAm), Faculty of Applied Sciences and Technology, Pagoh Higher Education Hub, Universiti Tun Hussein Onn Malaysia, 84600, Panchor, Johor, Malaysia

^e TriPrem i-Kohza, Malaysia-Japan International Institute Technology, Universiti Teknologi Malaysia, 54100, Kuala Lumpur, Malaysia

ARTICLE INFO

Keywords:

Bioactive glass
Fluoride
Compressive strength
Vickers microhardness

ABSTRACT

This paper outlines the fabrication of bioactive glass derived from waste eggshells as a source of calcium via the melt and water quenching method. The influence of the $\text{CaF}_2/\text{P}_2\text{O}_5$ ratio on the physical, structural and mechanical properties of bioglass samples was investigated. XRD confirmed the amorphous structure, while the presence of Si–O–Si, P–O, and C–O indicated the formation of bioglass samples. It was found that increasing CaF_2 content with appropriate P_2O_5 content could improve the mechanical properties of the bioglass. The increase in density can significantly impact the bioglass samples' compressive strength and vickers microhardness. The bioglass with $\text{CaF}_2/\text{P}_2\text{O}_5$ ratio of 6/4 possessed better properties, showing the optimal compressive strength (48.98 ± 0.11 MPa) and vickers microhardness (3.09 ± 0.07 GPa), which is compatible with the human enamel and commercial bioglass. Thus, the findings seem to contribute to a prospective cost-effective waste-derived bioglass system used in dental applications.

1. Introduction

Bioactive glasses are promising materials that have undergone substantial research over several decades [1,2]. The first invented bioactive glasses were named Bioglass® 45S5 by Larry Hench in the early 1970s [3]. It is a kind of biomaterial that can bond with hard and soft tissues by forming hydroxyapatite (HA) layer, mainly applied in biomedical and dental fields [4]. It has caught the attention of researchers over the years to study bioglass materials. Despite their outstanding bioactive characteristics, poor mechanical strength and fracture toughness are the main disadvantages limiting the use of non-load bearing applications [5]. According to the International Organization for Standardization 6872, a dental material needs to have better physical, chemical, biological and mechanical properties that are identical to natural teeth [6]. Therefore, several studies have been executed to enhance bioglasses' mechanical properties [7,8].

It is worth knowing that adding fluoride into bioglasses has a better

chance of promoting fluorapatite (FAP) formation instead of HA, a key element of enamel and dentine. FAP is less soluble in acidic environments and exhibits antibacterial characteristics, making it ideal for the dental fields [9]. Moreover, fluoride is also found to promote the density and mechanical strength of the glass system [10]. Hence, due to the fluoride's benefits, the studies on the influence of fluoride ions on bioglasses are still improving. Apart from that, P_2O_5 plays an essential role in enhancing the bioactivity of the bioglass. It allows the rapid apatite growth on the glass surface within the 2–10% range. The high content of P_2O_5 in the bioactive glass means that the content of P_2O_5 that is higher than 10 wt% will inhibit the bioactivity reaction of the bioglass [11]. Hence, in excess of P_2O_5 may inhibit the sign of bioactivity. However, previous researchers claimed that the P_2O_5 content that more than 7 wt % in the glass has a negative effect on the mechanical properties [12, 13]. To improve the mechanical properties and bioactive performance of the bioglass, this is challenging to choose the proper ratio of $\text{CaF}_2/\text{P}_2\text{O}_5$ to get the optimal properties for the novel bioglass composition.

* Corresponding author. Department of Physics, Faculty of Science, Universiti Putra Malaysia, UPM., 43400 Serdang, Selangor, Malaysia.

E-mail address: mhmzaid@upm.edu.my (M.H. Mohd Zaid).

<https://doi.org/10.1016/j.jpcs.2022.110991>

Received 6 June 2022; Received in revised form 9 August 2022; Accepted 1 September 2022

Available online 12 September 2022

0022-3697/© 2022 Elsevier Ltd. All rights reserved.

Improving the recycling rate of waste resources to develop valuable materials is an ongoing research focus worldwide [14]. Eggshells (EG) waste has great potential to reduce the cost of production while making the waste resource into more valuable material [15]. Doh and Chin reported that Malaysia is one of the biggest egg users globally, where EG waste has been disposed of in massive quantity in Malaysia [16]. It has also been ranked as the fifteenth major pollution problem in the food industry by the Environment Protection Agency [17]. ES waste contains 97–99% of calcium oxide after high sintering treatment of the eggshells. Hence, it has been suggested to use as a calcium source due to its low cost and availability [18].

The effect of the $\text{CaF}_2/\text{P}_2\text{O}_5$ ratio on the physical, structural and mechanical properties of the bioglass is expected to enhance and get the optimal ratio. The increase of the $\text{CaF}_2/\text{P}_2\text{O}_5$ ratio is expected to increase the densification and lead to an improvement in mechanical properties of the bioglass. Therefore, the current study aimed to fabricate the bioactive glass using EG waste as a source of calcium, with various ratios of $\text{CaF}_2/\text{P}_2\text{O}_5$ through the melt and water quenching method. The impact of $\text{CaF}_2/\text{P}_2\text{O}_5$ ratios of bioglass on the physical, structural and mechanical properties was experimentally investigated to determine their suitability for dental materials, which matches the mechanical properties of natural teeth.

2. Materials and methods

2.1. Glass synthesis

The starting materials of the bioactive glass system with the empirical formula $45\text{SiO}_2-25\text{CaO}-10\text{B}_2\text{O}_3-10\text{Na}_2\text{O}-(10-x)\text{P}_2\text{O}_5-x\text{CaF}_2$, where $x = 0, 2, 4, 6, 8$, and 10 wt%, were fabricated using melt and water quenching method. The eggshells (ES) waste has been chosen to replace the pure chemical CaO , while Na_2CO_3 was used for Na_2O . Firstly, the ES waste was cleaned and dried at room temperature. The ground dried ES was then sent for calcination process at 900°C for 2 h, at a heating rate of $10^\circ\text{C}/\text{min}$. During this process, the ES waste, CaCO_3 , will be converted into ES powder, CaO , with the release of CO_2 . X-ray fluorescence (XRF, ZSX Primus IV, Rigaku) was used to identify the elements and purity of the CaO produced in ES waste. After that, the ES powder was ground and sieved to $45\ \mu\text{m}$ and prepared for the mixing of other chemicals. A total of six chemicals included SiO_2 (Commercial), CaO (Extracted from ES waste), B_2O_3 (Acros Organics, 98%), Na_2CO_3 (Alfa Aesar, 99.5%), P_2O_5 (Sigma Aldrich), and CaF_2 (R&M Chemicals, 97%) were weighted following the empirical formula and mixed. The mixture was transferred into an alumina crucible for the melt and water quenching process at 1450°C for 2 h at a heating rate of $10^\circ\text{C}/\text{min}$. The water used to do quenching in this experiment is in room temperature. Next, the obtained glass frits were then crushed and sieved into $45\ \mu\text{m}$ particle size powder form. Last but not least, the bioglass samples with various $\text{CaF}_2/\text{P}_2\text{O}_5$ ratios were pressed into a 13 mm diameter size of pellet. The bioglass sample pellet will not undergo sintering and was sent for physical, structural, and mechanical characterization. The details of the investigated bioglass composition are revealed in Table 1.

Table 1
The bioglass composition with various $\text{CaF}_2/\text{P}_2\text{O}_5$ ratios in weight.%.

Composition	SiO_2	CaO	B_2O_3	Na_2O	P_2O_5	CaF_2
BG0F	45	25	10	10	10	–
BG1F	45	25	10	10	8	2
BG2F	45	25	10	10	6	4
BG3F	45	25	10	10	4	6
BG4F	45	25	10	10	2	8
BG5F	45	25	10	10	–	10

2.2. Glass characterization

The Archimedes method was used to determine the density measurement for bioglass samples. An average of five measurements were performed to get the density value provided with the accuracy of $\pm 0.001\ \text{g}/\text{cm}^3$. The formulation of density can be denoted as:

$$\rho_{\text{glass}} = \left(\frac{w_{\text{air}}}{w_{\text{air}} - w_{\text{water}}} \right) \rho_{\text{water}} \quad (1)$$

where w_{air} is the samples' weight in the air, w_{water} is the samples' weight in water, and ρ_{water} is the density of water which is $1.00\ \text{g}/\text{cm}^3$. The calculation of molar volume for bioglass samples can be expressed as:

$$V_m = \frac{M_T}{\rho_{\text{glass}}} \quad (2)$$

where M_T is the total molecular mass of the glass sample and ρ_{glass} is the density of glass. The accuracy of this measurement is $\pm 0.001\ \text{cm}^3/\text{mol}$.

The onset of glass transition temperature (T_g), crystallization onset temperature (T_x), glass crystallization temperature (T_c) and thermal stability factor (ΔT) of the glass sample were analyzed using differential scanning calorimetry (DSC) with a heating rate of $10^\circ\text{C}/\text{min}$ using thermogravimetric analyzer (model: Mettler Toledo, TGA/DSC 1 HT). DSC analysis was done on each sample placed on platinum base up to 900°C . X-ray diffraction (XRD, X'Pert PRO MPD diffractometer, PANalytical, Philips; Cu-K α radiation = $1.5406\ \text{\AA}$ at 40 kV and 40 mA was used), in the range of angle 20° – 80° to identify the amorphous nature structure of the bioglass samples. The absorption spectra of the samples were analyzed to determine the functional group using Fourier Transform Infrared (FTIR) spectrometer (Spectrum 100 series, PerkinElmer) in the Attenuated Total Internal Reflectance mode in the wavenumber ranging from 400 to $4000\ \text{cm}^{-1}$. FESEM model (FEI NOVA NanoSEM 230) was used to analyze the microstructure of the bioglass system with various $\text{CaF}_2/\text{P}_2\text{O}_5$ ratios. The samples were coated by platinum by using a spin coating machine to prevent electrostatic charge during the scanning process. The bioglass samples were observed with $5000\times$ magnification. The identification of weight percentage of C, O, F, Na, Si, P and Ca was measured by quantitative analysis.

To determine the mechanical properties of the bioglass samples, a compressive strength test (CST) and Vickers microhardness (HV) measurements were conducted. In this work, a compressive strength of bioglass is performed in cylinder dimension of $4.0\ \text{mm} \times 13.0\ \text{mm}$ pellet size. Compressive strength of the bioglass samples was performed by using Instron 3366 Dual Column Tabletop Universal Test System with $10\ \text{kN}$ load cell at a crosshead of $1\ \text{mm}/\text{min}$. The compressive strength value is calculated using the formula below:

$$\sigma_c = \frac{F}{\pi r^2} \quad (3)$$

where σ_c is the compressive strength, F is the force applied, and r is the radius of the cylinder pellet.

Vickers microhardness (HV) measurements were performed on the bioglass samples' surface by giving a load of $4.905\ \text{N}$ or HV 0.5 for 15 s. The measurements obtained five readings to get the average results on each various ratio bioglass samples. The calculation of the hardness test can be calculated using the formula as shown:

$$HV = 1.854 \left(\frac{2P \sin \theta}{D^2} \right) \quad (4)$$

where P is the applied load, D is the mean diagonal of the indentation (mm), and θ is the angle between the opposite faces of the diamond, which is 136° .

3. Results and discussion

3.1. XRF analysis

The purpose of XRF analysis is to confirm the chemical composition and the purity of the ES powder after calcination. The weight percentages of the ES composition are highlighted in Table 2. The table clearly shows that CaO produced in ES powder after calcination is 97.90%. Calcinated ES at 900 °C for 2 h is the optimal temperature and duration to get a higher percentage of CaO [19,20]. Hence, calcined ES is considered an excellent choice to replace the conventional CaO.

3.2. DSC analysis

The DSC curves obtained for the glass samples are presented in Table 3. All the DSC thermograms reveal a distinct onset of the glass transition temperature (T_g) and follow by crystallization onset temperature (T_x) and also glass crystallization peak temperature (T_c). The glass thermal stability (ΔT) also been measured. From Table 3, it can be concluded that the glass transition temperature, T_g , decreased gradually from 545 °C to 491 with the increase in CaF_2 concentration. The crystallization peak temperature also drops from 682 to 652 °C with the progress of CaF_2 addition in the glass matrix. However, the glass stability factor shows a very interesting trend with linearly increasing from 108 to 141 °C (until glass sample BG3F) and suddenly reduced to 138 °C with further addition of CaF_2 . From the trend, it can be concluded that the BG3F glass sample has the maximum thermal stability compared to other glass samples.

3.3. XRD analysis

XRD investigation is conducted on the bioglass system to confirm the amorphous glass structure. Fig. 1 clearly shows the XRD patterns of the bioglass (BG0F, BG1F, BG2F, BG3F, BG4F, and BG5F) with various $\text{CaF}_2/\text{P}_2\text{O}_5$ ratios. The graph reveals a broad hump shape for all the bioglass samples showing the characteristics of the amorphous glassy structure. It reflects the presence of short-range order in the bioglass samples; no sharp peak is observed. The result is agreed with ref. [21] claimed that the addition of CaF_2 content at below 10 wt% will not lead to the crystallization of the bioglass system, which will affect the bioactivity of the glass system.

3.4. FTIR analysis

The FTIR is a widely used analytical tool for discovering the functional groups of the materials. The FTIR spectra of bioglass with various ratios are presented in Fig. 2. Similar studies from different authors' previous work are gathered and compiled, as shown in Table 4. There are three characteristics mode of vibrations of Si-O bands of all the bioglass samples which can be noticed at ~ 440 , ~ 717 , and $\sim 998 \text{ cm}^{-1}$. The peak at $\sim 440 \text{ cm}^{-1}$ is assigned to the bending vibration mode of

Table 2

Weight percentages of the ES powder composition after calcination by XRF analysis.

Composition	Weight Percentage, %
CaO	97.9000
MgO	0.9030
Na_2O	0.1540
A_2O_3	0.1430
SiO_2	0.1400
P_2O_5	0.4040
SO_3	0.2200
K_2O	0.0436
Others	0.0924
Total	100.0000

Table 3

The values for T_g , T_x , T_c and ΔT for the bioglass system with various $\text{CaF}_2/\text{P}_2\text{O}_5$ ratios.

Glass sample	T_g (°C)	T_x (°C)	T_c (°C)	ΔT (°C)
BG0F	545	653	682	108
BG1F	519	650	677	131
BG2F	509	645	671	136
BG3F	496	637	662	141
BG4F	493	632	657	139
BG5F	491	629	652	138

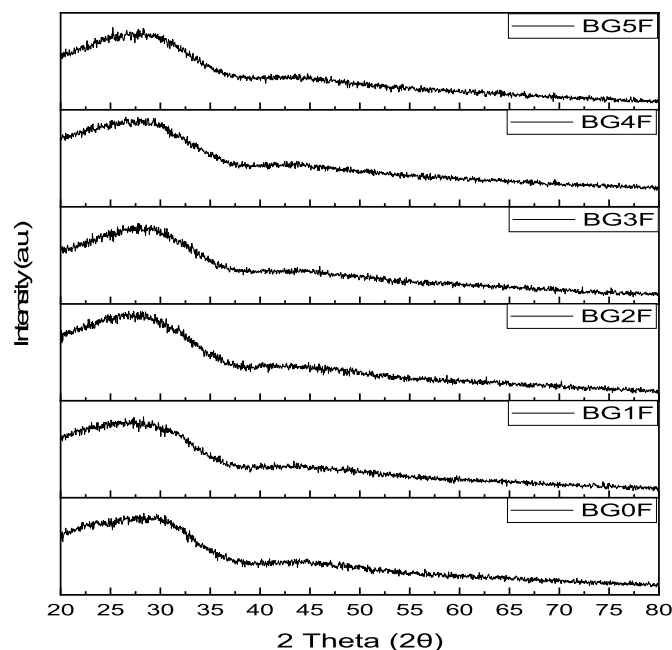


Fig. 1. XRD patterns of the bioglass system with various $\text{CaF}_2/\text{P}_2\text{O}_5$ ratios.

Si-O-Si. The bands at $\sim 717 \text{ cm}^{-1}$ and $\sim 998 \text{ cm}^{-1}$ correspond to the Si-O-Si stretching vibration and Si-O-Si asymmetric stretching modes. These findings are similar to the de Siqueira and the co-workers in Ref. [22]. Moreover, the absorption peak at $\sim 552 \text{ cm}^{-1}$ is attributed to the P-O bending mode, shown in BG0F to BG3F. This band starts to disappear with the increase of $\text{CaF}_2/\text{P}_2\text{O}_5$ ratios. Another band situated in $\sim 1401 \text{ cm}^{-1}$ is attributed to the C-O stretching vibration mode. The appearance of the carbonate group may be related to the dissolving of carbon dioxide from the ambient temperature from the decomposition of calcium carbonate and sodium carbonate used in the glass system [23].

3.5. FESEM/EDX analysis

FESEM micrographs is used to describe the microstructure and morphology of the bioglass while EDX spectra is to determine the quantitative chemical composition of the bioglass with various ratios. Fig. 3 depicts the FESEM micrographs of bioglass system at 5000 \times magnification and Fig. 4 presents the EDX spectra of the bioglass system. The figure shows non-uniform particle distribution by the formation of irregular shapes and sharp particle edge in all the bioglass samples. The results indicate the amorphous glassy structure which can confirmed by the XRD results.

Besides, the EDX analysis in the figure confirmed the appearance of the weight percentage of each element in the bioglass. The bioglass sample BG0F contains the element P with 2.22 wt%. However, with the increase of $\text{CaF}_2/\text{P}_2\text{O}_5$ ratios to BG4F, the element P decreases to 0.27 wt % while BG5F does not contains element P. Furthermore, the weight

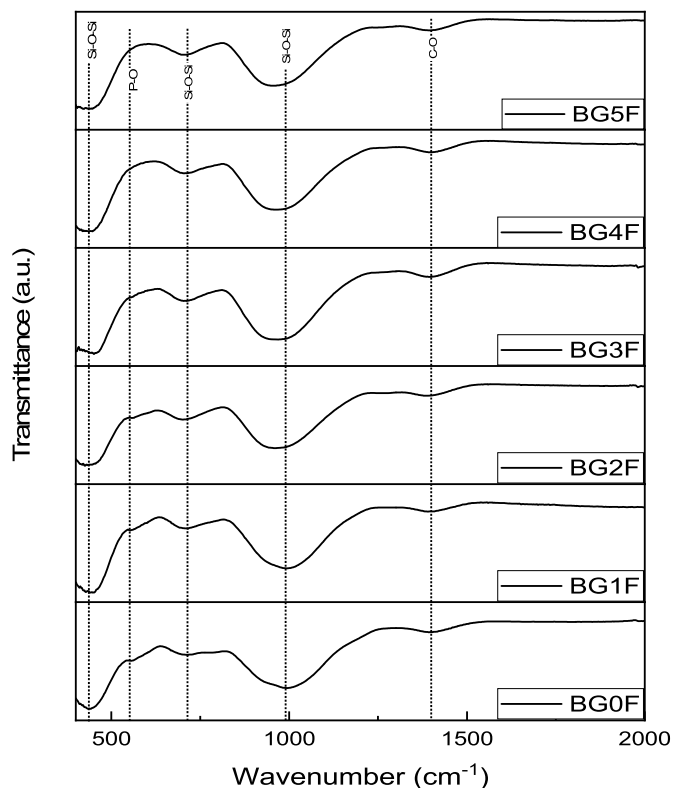


Fig. 2. FTIR spectra of the bioglass system with various $\text{CaF}_2/\text{P}_2\text{O}_5$ ratios.

Table 4

FTIR spectral band assigned to the vibrational modes.

Wavenumbers (cm^{-1})	Assignment of vibrational mode	Reference
~440	Si-O-Si bending mode	[22]
~552	P-O bending mode	[24]
~717	Si-O-Si stretching vibration mode	[25]
~956–998	Si-O-Si asymmetric stretching mode	[26]
~1401	C-O stretching mode	[27]

percentage of F increase from BG1F with 1.70 wt% to BG5F with 7.08 wt % with the increase of $\text{CaF}_2/\text{P}_2\text{O}_5$ ratios.

3.6. Density and molar volume analysis

Density measurement is a crucial variable to identify the changes in the glass network structure. Fig. 5 depicts the density and molar volume of the bioglass system with various $\text{CaF}_2/\text{P}_2\text{O}_5$ ratios. From the figure, the density increases from $2.126 \pm 0.001 \text{ g/cm}^3$ to $2.168 \pm 0.002 \text{ g/cm}^3$ with the increase in $\text{CaF}_2/\text{P}_2\text{O}_5$ ratios. The increase in density is ascribed to the structural rearrangement of the bioglass networks with the addition of fluoride concentration. Alternatively, it might be related to the high density of CaF_2 (3.180 g/cm^3) compared to P_2O_5 (2.300 g/cm^3). Therefore, this phenomenon increased the glass density, which agrees with Naresh and co-workers [28]. However, there is a drop in density resulting in BG4F and BG5F. Raising the fluoride amount further will have a detrimental effect since excess CaF_2 would cause the glass network to become defective, lead to a less dense silicate system and impair the hardness of the glass system [29]. Apart from that, molar volume is inversely proportional to density. Hence, the graph in molar volume shows a decreasing diagram with the increase in $\text{CaF}_2/\text{P}_2\text{O}_5$ ratios. In this research, the molar volume of the bioglass system decreased from $38.968 \pm 0.480 \text{ cm}^3/\text{mol}$ to $29.207 \pm 0.100 \text{ cm}^3/\text{mol}$. It might be attributed to the changes in atomic structure that disturb the silicate glass system. The addition of CaF_2 will modify the silicate glass; more non-bridging oxygen is created while forming new bonding between the fluoride ions and oxygen atoms to create bridging oxygen bonds. As a result, it improves the glass' compactness, leading to an increase in density and a decrease in molar volume [30,31].

3.7. Compressive strength analysis

The compressive strength test is crucial to evaluate the mechanical properties of the dental material, especially during the mastication process [32]. The average applied load range during chewing different kinds of food is from 6 to 440 N [33]. The compressive strength of bioglass system with various $\text{CaF}_2/\text{P}_2\text{O}_5$ ratios is presented in Fig. 6. With the increase of CaF_2 content, the compressive strength increases from $46.80 \pm 0.15 \text{ MPa}$ to $48.98 \pm 0.11 \text{ MPa}$ first and then decreases to $47.01 \pm 0.05 \text{ MPa}$, which has a similar trend with density. The results obtained from BG0F to BG5F are considerably higher than the commercial 45S5 bioglass ceramics ($\sim 37 \text{ MPa}$) [34]. Among the bioglass

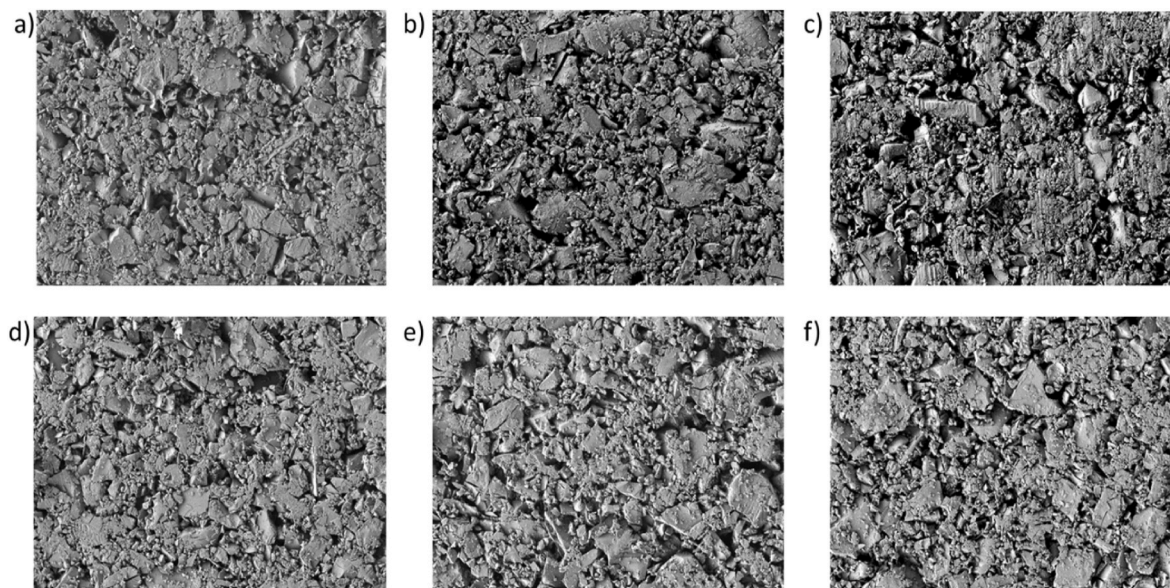


Fig. 3. FESEM micrographs of bioglass system at $5000\times$ magnification for (a) BG0F, (b) BG1F, (c) BG2F, (d) BG3F, (e) BG4F and (f) BG5F.

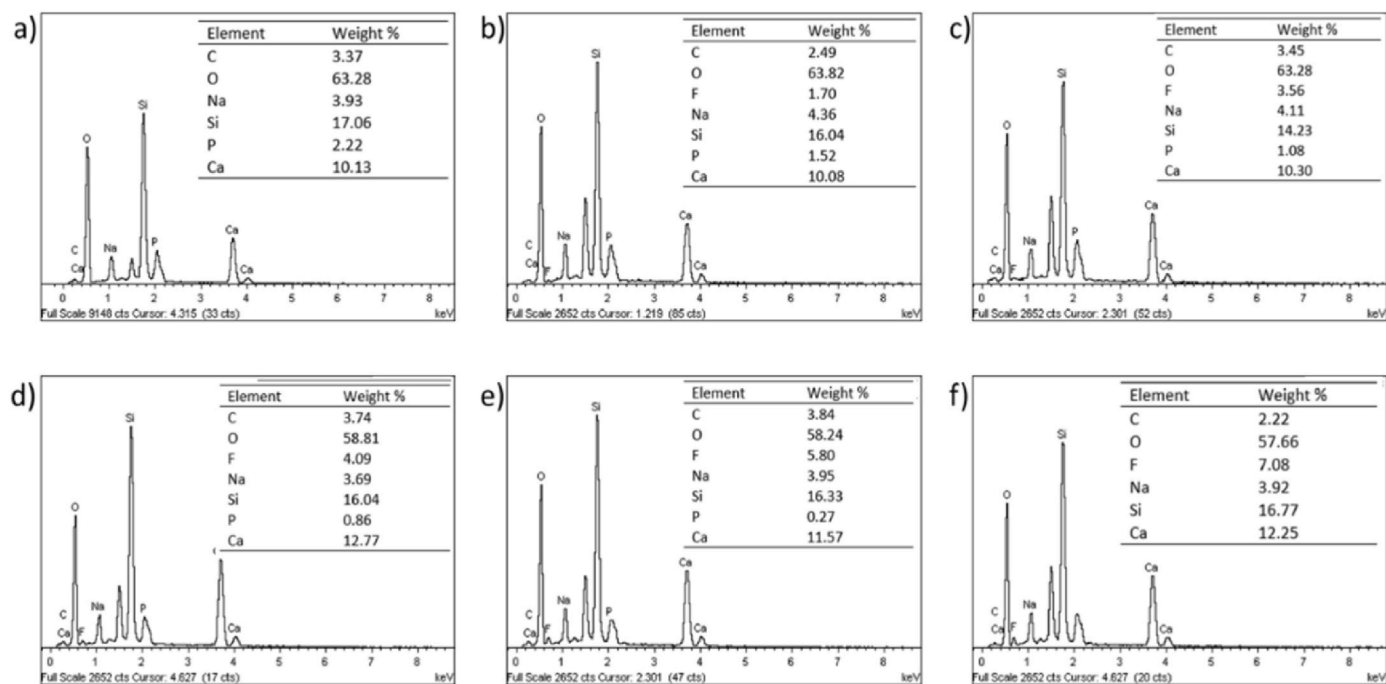


Fig. 4. EDX spectra of bioglass system for (a) BG0F, (b) BG1F, (c) BG2F, (d) BG3F, (e) BG4F, and (f) BG5F.

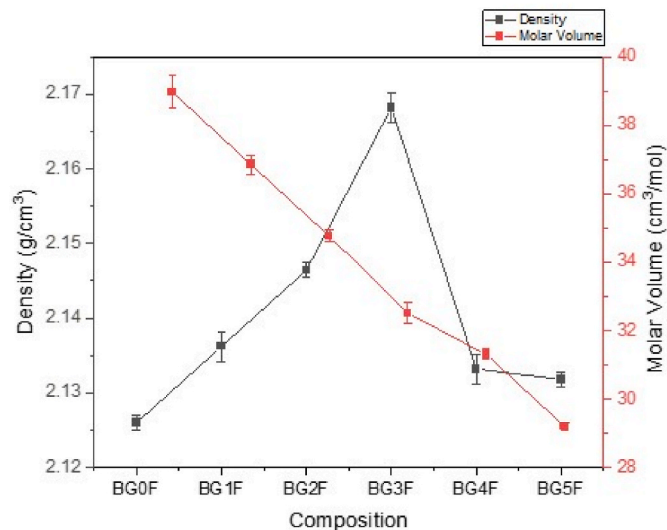


Fig. 5. The density and molar volume of the bioglass system with various $\text{CaF}_2/\text{P}_2\text{O}_5$ ratios.

samples, BG3F achieve the optimal compressive strength performance, 48.98 ± 0.11 MPa. The addition of CaF_2 content with control of P_2O_5 would lead to the compactness of the structure of the bioglass structure [35,36]. Nevertheless, BG4F and BG5F showing poor compressive strength results might be caused by the excess CaF_2 in the bioglass system, affecting the mechanical properties of the final products [37, 38].

3.8. Vickers microhardness analysis

Vickers microhardness test is another significant mechanical feature used to measure the hardness of dental materials in long-term success as it can determine the hardness of the soft and hard surface materials with higher accuracy [39]. A higher hardness value would benefit the dental

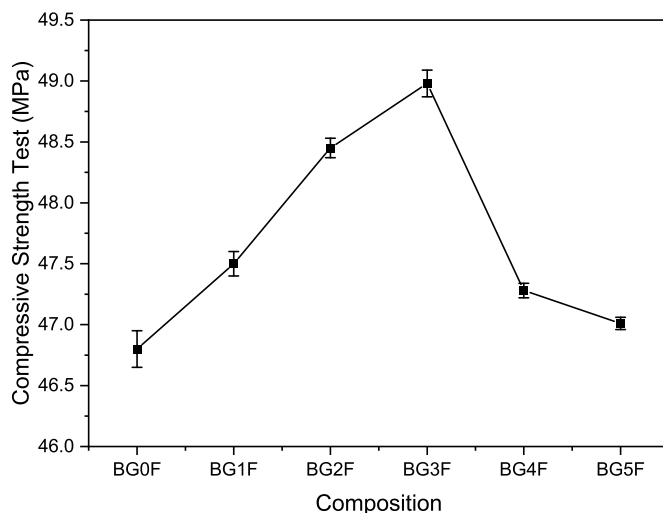


Fig. 6. The compressive strength of bioglass system with various $\text{CaF}_2/\text{P}_2\text{O}_5$ ratios.

materials during mastication. Fig. 7 presents the Vickers microhardness of bioglass system with various $\text{CaF}_2/\text{P}_2\text{O}_5$ ratios. A similar pattern can be seen with density and compressive strength results. The results reveal an increasing trend for BG0F to BG3F, with the value from 2.00 ± 0.07 GPa to 3.09 ± 0.07 GPa. There is a decreasing trend for BG4F to BG5F, with the value from 3.04 ± 0.05 GPa to 3.03 ± 0.03 GPa. Therefore, bioglass BG3F with $\text{CaF}_2/\text{P}_2\text{O}_5$ ratio of 6/4 possesses the optimal microhardness value compared to the human enamel, which is approximately in the range of 3–5 GPa [40]. They also claimed that fluoride additive in the bioglass system enhanced the microhardness suitable for dental applications. The microhardness of commercial 45S5 bioglass, 0.148 GPa, has improved to 1.083 GPa with the incorporation of CaF_2 [41]. This work aims to improve the mechanical properties of the novel bioactive glass system in terms of dental application.

The addition of P_2O_5 content in the bioglass system can improve the bioactivity properties of the glass by forming the hydroxyapatite (HA)

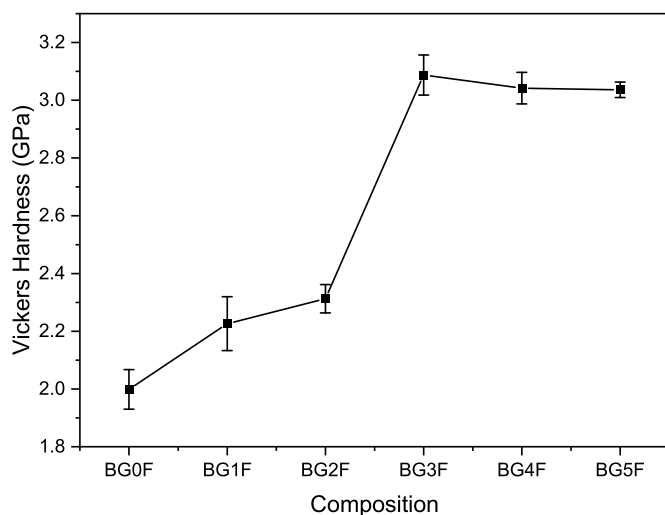


Fig. 7. Vickers microhardness of bioglass system with various CaF₂/P₂O₅ ratios.

that can bond to hard and soft tissues. However, for the mechanical sides, the high content of P₂O₅ will affect the mechanical properties of the bioglass system as it will increase the porosity and decrease in grain size of the crystal. On the other hand, the addition of CaF₂ content in the bioglass system results in the densification and compactness of the glass system, leading to the improvement of mechanical properties comparable with the human enamel. The formation of fluorapatite (FAP) in the bioglass is preferable as fluoride is the key agent in preventing the dental caries by enhancing the remineralization and inhibiting the demineralization. FAP is one of the main components of enamel and dentin, which is more beneficial to apply in dental applications. Hence, to improve the mechanical properties of the bioglass glass system while maintaining the bioactivity properties, the CaF₂/P₂O₅ ratio will be considered to get the optimal results and further studies for the bioactivity properties.

4. Conclusion

The cost-effective bioactive glass with various CaF₂/P₂O₅ ratios has been successfully fabricated throughout this work by utilizing the eggshells waste as a source of calcium via the melt-quenching technique. The XRF analysis showed the significant oxides in the calcined eggshells with high purity was CaO. The XRD and FTIR results confirmed the amorphous glassy structure of all the bioglass samples. Meanwhile, the presence of Si–O–Si, P–O, and C–O in the bioglass samples showed the formation of the bioglass system. The density increases while the molar volume decreases with the increase in CaF₂/P₂O₅ ratios. The increase in density can greatly impact the compressive strength and vickers microhardness of the bioglass samples. BG3F with a CaF₂/P₂O₅ ratio of 6/4 exhibited optimal compressive strength, 48.98 ± 0.11 MPa, and microhardness, 3.09 ± 0.07 GPa among the bioglass samples. Thus, this study proposes a novel strategy for fabricating bioglass as promising dental materials by using waste resources.

Credit authorship contribution statement

Zhi Wei Loh: Conceptualization, Methodology, Software, Formal analysis, Investigation, Data Curation, Writing - Original Draft, Visualization. **Mohd Hafiz Mohd Zaid:** Conceptualization, Methodology, Formal analysis, Data Curation, Writing - Original Draft, Supervision, Project administration, Funding acquisition. **Mohd Mustafa Awang Kechik, Yap Wing Fen:** Formal analysis, Data Curation, Writing - Review & Editing, Supervision. **Data Curation, Writing - Review & Editing. Yazid Yaakob, Mohd Zul Hilmi Mayzan, Shahira Liza:** Methodology, Software, Formal analysis, Data Curation. **Wei Mun Cheong:**

Conceptualization, Methodology, Software, Formal analysis, Investigation.

Declaration of competing interest

The authors declare that they have no known competing financial interests or personal relationships that could have appeared to influence the work reported in this paper.

Data availability

Data will be made available on request.

Acknowledgments

This research was supported by the Universiti Putra Malaysia through the Geran Putra Berimpak (GP-GPB/2021/9702600) for this research work.

References

- [1] F. Sharifianjazi, M. Moradi, A. Abouchenari, A.H. Pakseresht, A. Esmailkhanian, M. Shokouhimehr, M. Shahedi Asl, Effects of Sr and Mg dopants on biological and mechanical properties of SiO₂-CaO-P₂O₅ bioactive glass, *Ceram. Int.* 46 (2020) 22674–22682.
- [2] N.A.A. Rahman, K.A. Matori, M.H.M. Zaid, N. Zainuddin, S.A. Aziz, M.Z.A. Khiri, R. A. Jilil, W.N.W. Jusoh, Fabrication of Alumino-Silicate-Fluoride based bioglass derived from waste clam shell and soda lime silica glasses, *Results Phys.* 12 (2019) 743–747.
- [3] L.L. Hench, The story of Bioglass, *J. Mater. Sci. Mater. Med.* 17 (2006) 967–978.
- [4] M. Zine Elabidine, M.A. Cherbib, I. Khattech, A. Bechrifa, K. Schuhladden, D. S. Brauer, A.R. Boccaccini, Calorimetric approach to assess the apatite-forming capacity of bioactive glasses, *J. Non-Cryst. Solids* 550 (2020).
- [5] C. Moequot, N. Attik, N. Pradelle-Plasse, B. Grosgeat, P. Colon, Bioactivity assessment of bioactive glasses for dental applications: a critical review, *Dent. Mater.* 36 (2020) 1116–1143.
- [6] K. Dimitriadis, D.U. Tulyaganov, S. Agathopoulos, Development of novel alumina-containing bioactive glass-ceramics in the CaO-MgO-SiO₂ system as candidates for dental implant applications, *J. Eur. Ceram. Soc.* 41 (2021) 929–940.
- [7] Y. Seo, T. Goto, H. Nishida, S.H. Cho, A. Zarkov, T. Yamamoto, T. Sekino, Low-temperature mineralization sintering process for fabrication of fluoridated hydroxyapatite-containing bioactive glass, *J. Ceram. Soc. Japan.* 128 (2020) 783–789.
- [8] H.E. Skalleveid, D. Rokaya, Z. Khurshid, M.S. Zafar, Bioactive glass applications in dentistry, *Int. J. Mol. Sci.* 20 (2019) 1–24.
- [9] S. Prasad, S. Ganiseti, A. Jana, S. Kant, P.K. Sinha, S. Tripathy, K. Illath, T. G. Ajithkumar, K. Annapurna, A.R. Allu, K. Biswas, Elucidating the effect of CaF₂ on structure, biocompatibility and antibacterial properties of S53P4 glass, *J. Alloys Compd.* 831 (2020), 154704.
- [10] H.C. Li, D.G. Wang, J.H. Hu, C.Z. Chen, Crystallization, mechanical properties and in vitro bioactivity of sol-gel derived Na₂O-CaO-SiO₂-P₂O₅ glass-ceramics by partial substitution of CaF₂ for CaO, *J. Sol. Gel Sci. Technol.* 67 (2013) 56–65.
- [11] S.N.F.S. Adam, F. Zainuddin, A.F. Osman, Effect of varying phosphate content on the structure and properties of sol-gel derived SiO₂-CaO-P₂O₅ bio-glass, *J. Phys. Conf. Ser.* 2080 (2021).
- [12] N.A. Al-eesa, F.S.L. Wong, A. Johal, R.G. Hill, Fluoride containing bioactive glass composite for orthodontic adhesives – ion release properties, *Dent. Materials* 33 (2017) 1324–1329.
- [13] V.K. Marghussian, A. Sheikh-Mehdi Mesgar, Effects of composition on crystallization behaviour and mechanical properties of bioactive glass-ceramics in the MgO-CaO-SiO₂-P₂O₅ system, *Ceram. Int.* 26 (2000) 415–420.
- [14] C. Xu, M. Nasrollahzadeh, M. Selva, Z. Issaabadi, R. Luque, Waste-to-wealth: biowaste valorization into valuable bio(nano)materials, *Chem. Soc. Rev.* 48 (2019) 4791–4822.
- [15] L.Z. Wei, C.W. Mun, H.M.H. Zakaly, S.A.M. Issa, M.H.M. Zaid, Influence of sintering duration on crystal phase and optical band gap of Mn³⁺-doped willemite-based glass-ceramics, *J. Electron. Mater.* 51 (2022) 1163–1168.
- [16] S.I. Doh, S.C. Chin, Eggshell Powder: Potential Filler in Concrete, 8th MUCET, 2014, pp. 1–5.
- [17] M. Waheed, M. Yousaf, A. Shehzad, M. Inam-Ur-Raheem, M.K.I. Khan, M.R. Khan, N. Ahmad, Abdullah, R.M. Aadil, Channelling eggshell waste to valuable and utilizable products: a comprehensive review, *Trends Food Sci. Technol.* 106 (2020) 78–90.
- [18] C. Harripersadth, P. Musonge, Y. Makarfi Isa, M.G. Morales, A. Sayago, The application of eggshells and sugarcane bagasse as potential biomaterials in the removal of heavy metals from aqueous solutions, *S. Afr. J. Chem. Eng.* 34 (2020) 142–150.
- [19] I.H. Alsohaimi, A.M. Nassar, T.A. Seaf Elnasr, B. amar Cheba, A novel composite silver nanoparticles loaded calcium oxide stemming from egg shell recycling: a

- potent photocatalytic and antibacterial activities, *J. Clean. Prod.* 248 (2020), 119274.
- [20] R. Rohim, R. Ahmad, N. Ibrahim, N. Hamidin, C.Z. Azner Abidin, Characterization of calcium oxide catalyst from eggshell waste, *Adv. Environ. Biol.* 8 (2014) 35–38.
- [21] R. Abdul Jalil, K. Amin Matori, M.H. Mohd Zaid, N. Zainuddin, M.Z. Ahmad Khiri, N.A. Abdul Rahman, W.N. Wan Jusoh, E. Kul, A study of fluoride-containing bioglass system for dental materials derived from clam shell and soda lime silica glass, *J. Spectrosc.* 2020 (2020).
- [22] L. de Siqueira, T.M.B. Campos, S.E.A. Camargo, G.P. Thim, E.S. Trichês, Structural, crystallization and cytocompatibility evaluation of the 45S5 bioglass-derived glass-ceramic containing niobium, *J. Non-Cryst. Solids* 555 (2021).
- [23] N.F.B. Pallan, K.A. Matori, M. Hashim, R.S. Azis, N. Zainuddin, N.F.B. Pallan, F. M. Idris, I.R. Ibrahim, L.C. Wah, S.N.A. Rusly, N. Adnin, M.Z.A. Khiri, Z.N. Alassan, N. Mohamed, M.H.M. Zaid, Effects of different sintering temperatures on thermal, physical, and morphological of $\text{SiO}_2\text{-Na}_2\text{O-CaO-P}_2\text{O}_5$ based glass-ceramic system from vitreous and ceramic wastes, *Sci. Sinter.* 51 (2019) 377–387.
- [24] D. Kaur, M.S. Reddy, O.P. Pandey, Synthesis, characterization, drug loading and in-vitro bioactivity studies of rice husk derived $\text{SiO}_2\text{-P}_2\text{O}_5\text{-MgO-CaO-SrO}$ bio-active glasses, *J. Drug Deliv. Sci. Technol.* (2020) 1–10.
- [25] B. Karakuzu-Ikizler, P. Terzioğlu, Y. Basaran-Elalmis, B.S. Tekerek, S. Yücel, Role of magnesium and aluminum substitution on the structural properties and bioactivity of bioglasses synthesized from biogenic silica, *Bioact. Mater.* 5 (2020) 66–73.
- [26] R.M. Rad, A.Z. Alshemary, Z. Evis, D. Keskin, K. Altunbaş, A. Tezcaner, Structural and biological assessment of boron doped bioactive glass nanoparticles for dental tissue application, *Ceram. Int.* 44 (2018), 13453.
- [27] V. Uskoković, G. Abuna, P. Ferreira, V.M. Wu, L. Gower, F.C.P. Pires-de-Souza, R. M. Murata, M.A.C. Sinhoreti, S. Geraldeli, Synthesis and characterization of nanoparticulate niobium- and zinc-doped bioglass-ceramic/chitosan hybrids for dental applications, *J. Sol. Gel Sci. Technol.* 97 (2021) 245–258.
- [28] P. Naresh, N. Narsimlu, C. Srinivas, M. Shareefuddin, K. Siva Kumar, Ag_2O doped bioactive glasses: an investigation on the antibacterial, optical, structural and impedance studies, *J. Non-Cryst. Solids* 549 (2020).
- [29] S.Z. Zhao, X.Y. Zhang, B. Liu, J.J. Zhang, H.L. Shen, S.G. Zhang, Preparation of glass-ceramics from high-chlorine MSWI fly ash by one-step process, *Rare Met.* 40 (2021) 3316–3328.
- [30] N. Effendy, S.H. Ab Aziz, H. Mohamed Kamari, M.H. Mohd Zaid, S.A. Abdul Wahab, Ultrasonic and artificial intelligence approach: elastic behavior on the influences of ZnO in tellurite glass systems, *J. Alloys Compd.* 835 (2020) 1–11.
- [31] R.F. Muniz, V.O. Soares, G.H. Montagnini, A.N. Medina, M.L. Baesso, Thermal, optical and structural properties of relatively depolymerized sodium calcium silicate glass and glass-ceramic containing CaF_2 , *Ceram. Int.* 47 (2021) 24966–24972.
- [32] R.A.S. Alatawi, N.H. Elsayed, W.S. Mohamed, Influence of hydroxyapatite nanoparticles on the properties of glass ionomer cement, *J. Mater. Res. Technol.* 8 (2019) 344–349.
- [33] L. Fu, H. Engqvist, W. Xia, Glass-ceramics in dentistry: a review, *Materials* 13 (2020) 1–23.
- [34] M. Araújo, M. Miola, G. Baldi, J. Perez, E. Verné, Bioactive glasses with low Ca/P ratio and enhanced bioactivity, *Materials* 9 (2016) 1–14.
- [35] R.P. Vikash Kumar Vyasa, Arepalli Sampath Kumara, Akher Alia, Sunil Prasada, Pradeep Srivastava, Sarada Prasanna Mallick, Md Ershada, Saryoo Prasad Singha, Assessment of Nickel Oxide Substituted Bioactive Glass-Ceramic on in Vitro Bioactivity and Mechanical Properties, 2016, p. 14.
- [36] G. Kaur, V. Kumar, F. Bairo, J.C. Mauro, G. Pickrell, I. Evans, O. Bretcanu, Mechanical properties of bioactive glasses, ceramics, glass-ceramics and composites: state-of-the-art review and future challenges, *Mater. Sci. Eng. C* 104 (2019) 1–14.
- [37] A.M. Deliormanlı, M. Ensoylu, S.A.M. Issa, W. Elshami, A.M. Al-Baradi, M.S. Al-Buriah, H.O. Tekin, WS_2 /bioactive glass composites: fabrication, structural, mechanical and radiation attenuation properties, *Ceram. Int.* 47 (2021) 29739–29747.
- [38] T. Rezaee, M.L. Bouxsein, L. Karim, Increasing fluoride content deteriorates rat bone mechanical properties, *Bone* 136 (2020), 115369.
- [39] N.D. Yanikoglu, R.E. Sakarya, Test methods used in the evaluation of the structure features of the restorative materials: a literature review, *J. Mater. Res. Technol.* 9 (2020) 9720–9734.
- [40] M. Montazerian, E.D. Zanotto, Bioactive and inert dental glass-ceramics, *J. Biomed. Mater. Res., Part A* 105 (2017) 619–639.
- [41] F.A. Shah, Fluoride-containing bioactive glasses: glass design, structure, bioactivity, cellular interactions, and recent developments, *Mater. Sci. Eng. C* 58 (2016) 1279–1289.